$1/f$ spectrum and memory function analysis of solvation dynamics in a room-temperature ionic liquid

Daun Jeong,[1] M. Y. Choi,[2,3] YounJoon Jung,[1,*] and Hyung J. Kim[4]

[1]*Department of Chemistry, Seoul National University, Seoul 151-747, Korea*
[2]*Department of Physics and Astronomy, Seoul National University, Seoul 151-747, Korea*
[3]*Asia-Pacific Center for Theoretical Physics, Pohang University of Science and Technology, Pohang 790-784, Korea*
[4]*Department of Chemistry, Carnegie Mellon University, Pittsburgh, PA 15213, U.S.A.*
(Dated: March 31, 2008)

To understand the non-exponential relaxation associated with solvation dynamics in the ionic liquid 1-ethyl-3-methylimidazolium hexafluorophosphate, we study power spectra of the fluctuating Franck-Condon energy gap of a diatomic probe solute via molecular dynamics simulations. Results show $1/f$ dependence in a wide frequency range over 2 to 3 decades, indicating distributed relaxation times. We analyze the memory function and solvation time in the framework of the generalized Langevin equation using a simple model description for the power spectrum. It is found that the crossover frequency toward the white noise plateau is directly related to the time scale for the memory function and thus the solvation time. Specifically, the low crossover frequency observed in the ionic liquid leads to a slowly-decaying tail in its memory function and long solvation time. By contrast, acetonitrile characterized by a high crossover frequency and (near) absence of $1/f$ behavior in its power spectra shows fast relaxation of the memory function and single-exponential decay of solvation dynamics in the long-time regime.

I. INTRODUCTION

Solvation dynamics in room-temperature ionic liquids (RTILs) have received intensive theoretical[1,2,3,4,5,6,7,8,9] and experimental attention recently.[10,11,12,13,14,15,16] The collective influence of the solvent in the presence of an optically-active probe solute is usually monitored via various dynamic electronic spectroscopies and described in terms of time-dependent fluctuations and relaxation of the Franck-Condon (FC) transition energy of the solute in solution. Often observed in RTILs is biphasic relaxation comprised of ultrafast sub-picosecond dynamics and ensuing non-exponential decay. Short-time solvation dynamics, arising mainly from small-amplitude inertial translational motions of solvent ions, make a substantial contribution to overall solvent relaxation despite their high viscosity,[4,6] and thus can play an important role in reaction dynamics[17] in RTILs. The subsequent relaxation, attributed to diffusive dynamics, involves cooperative movement of ions and accompanying structural relaxation.

A spectral analysis of the FC energy gap, which is equivalent to analyzing its time correlation function, is useful for investigating dynamics over various time scales. Of particular interest are long-time fluctuations that often result in non-exponential relaxation. For instance, $1/f$ behavior for long-time fluctuations in water[18] and liquid silica[19] has been reported. Defect fluctuations in a disordered two-dimensional liquid also exhibit $1/f$ spectra, suggesting that system dynamics are heterogeneous.[20] Slow relaxation in these systems indicates that the structural memory persists for a long time in spite of the fast inertial motion of solvent molecules.

In the generalized Langevin equation (GLE) description of solvation dynamics,[21,22] the time-dependent friction plays the role of a memory function. The temporal behavior of the memory function for a variety of liquid systems has been analyzed via numerical transforms of appropriate time correlation functions[4,21,23,24] and a self-consistency method.[25] The memory function couched in terms of radial distribution functions has also been studied numerically.[26] Memory functions thus analyzed have two general characteristics in common, a rapid decay within the first few hundred femtoseconds of relaxation and a long tail thereafter. The former among these features originates mainly from short-time collisions via fast inertial motions of molecules in liquids. The residual memory effect which can last for a prolonged period governs the long-time behavior of relaxation dynamics. In solvation dynamics, the overall friction given by the integration of the memory function including its long-time tail is directly related to the solvation time.

In this study, we investigate the power spectra of the FC energy gap in the room-temperature ionic liquid, 1-ethyl-3-methylimidazolium hexafluorophosphate ($EMI^+PF_6^-$), employing a diatomic probe solute via molecular dynamics (MD) computer simulations. Among others, $1/f$ dependence and crossover to the white noise are observed in the low frequency region of the spectra. The latter represents the onset of normal diffusion, which marks the escape from the subdiffusive regime in the intermediate time scale corresponding to the $1/f$ region.[27] In the GLE description of solvation dynamics, the memory function can be expressed conveniently in terms of the power spectrum of the FC energy gap. Using a simple model description for the power spectrum, we compute the memory function and confirm that the crossover frequency determines the time scale of the memory function decay and is inversely proportional to the solvation time.

This paper is organized as follows: In Sec. II, we briefly review solvation dynamics, its GLE description and power spectrum analysis. In Sec. III, simulation

methods are described. MD results for the time correlation functions and power spectra are presented in Sec. IV, while the memory functions are analyzed by using a model description in Sec. V. Concluding remarks are offered in Sec. VI.

II. SOLVATION DYNAMICS

In this section we review briefly the time correlation function of the FC energy gap and its power spectrum, and the GLE approach to equilibrium solvation dynamics. We assume that the probe solute is characterized by an active electronic state a and a reference electronic state r as in previous MD studies.[4,7,8] For a given solvent configuration, the FC energy associated with the $a \rightarrow r$ transition of the solute is given by

$$\Delta E_{a \rightarrow r} = E_r - E_a , \qquad (1)$$

where $E_{a,r}$ denotes the total energy of the solute-solvent system with the solute in state a and r, respectively.

We consider the equilibrium solvation dynamics, characterized by the normalized time correlation function

$$C_{a/r}(t) \equiv \frac{\langle \delta \Delta E_{a \rightarrow r}(0) \delta \Delta E_{a \rightarrow r}(t) \rangle}{\langle (\delta \Delta E_{a \rightarrow r})^2 \rangle} , \qquad (2)$$

where $\langle \cdots \rangle$ denotes the equilibrium ensemble average in the presence of the a-state solute and $\delta \Delta E_{a \rightarrow r} \equiv \Delta E_{a \rightarrow r} - \langle \Delta E_{a \rightarrow r} \rangle$ depending on time t. Henceforth the subscripts representing the solute electronic states are suppressed for brevity.

The time correlation function is conveniently described by the GLE,[21,22] derived via the Mori-Zwanzig projection[28,29] onto a set of dynamical variables $\{\delta \Delta E, \delta \Delta \dot{E}\}$:

$$\delta \Delta \ddot{E}(t) = -\omega_s^2 \, \delta \Delta E(t) - \int_0^t dt' \, \zeta(t - t') \, \delta \Delta \dot{E}(t') + R(t), \qquad (3)$$

where the solvent frequency $\omega_s \equiv \sqrt{\langle (\delta \Delta \dot{E})^2 \rangle \langle (\delta \Delta E)^2 \rangle^{-1}}$ characterizes inertial dynamics of ΔE,[21] and the time-dependent friction (i.e., the memory function) $\zeta(t)$ and the random force $R(t)$ (scaled by the inertia associated with $\delta \Delta E$ dynamics) are related via the fluctuation-dissipation theorem

$$\zeta(t) = \frac{\langle R(0) R(t) \rangle}{\langle (\delta \Delta \dot{E})^2 \rangle} . \qquad (4)$$

The equilibrium time-correlation function $C(t)$ satisfies

$$\ddot{C}(t) = -\omega_s^2 C(t) - \int_0^t dt' \zeta(t - t') \dot{C}(t') . \qquad (5)$$

Taking the Laplace transform

$$\tilde{C}(z) = \int_0^\infty \exp(-zt) \, C(t) dt , \qquad (6)$$

we obtain

$$\tilde{C}(z) = \left(z + \frac{\omega_s^2}{z + \tilde{\zeta}(z)} \right)^{-1} , \qquad (7)$$

which shows that the solvation time $\tau_{\text{solv}} \equiv \int_0^\infty C(t) dt = \tilde{C}(0)$ is governed by $\tilde{\zeta}(0)$ and ω_s^2.

The normalized power spectrum of the FC energy gap $\delta \Delta E_{a \rightarrow r}$ is defined to be

$$S_{a/r}(f) \equiv \lim_{T \rightarrow \infty} \frac{1}{T} \left| \int_{-T/2}^{T/2} \frac{\delta \Delta E_{a \rightarrow r}(t)}{\sqrt{\langle (\delta \Delta E_{a \rightarrow r})^2 \rangle}} e^{2\pi i f t} dt \right|^2 , \qquad (8)$$

which corresponds to the Fourier transform of the (normalized) correlation function $C(t)$, according to the well-known Wiener-Khintchine theorem.[30] Namely, the correlation function, which is real, relates to the power spectrum via

$$C(t) = 2\pi \int_{-\infty}^{\infty} df S(f) \cos 2\pi f t . \qquad (9)$$

Because of the discrete nature of sampling in simulations, we use the discretized form of the power spectrum:[31]

$$S(f_k) = \frac{\Delta t}{N} \left| \sum_{n=0}^{N-1} \frac{\delta \Delta E_n}{\sqrt{\langle (\delta \Delta E)^2 \rangle}} e^{2\pi i n k / N} \right|^2 , \qquad (10)$$

where N is the number of samples, $f_k (\equiv k/N\Delta t)$ is the kth frequency ($k = 0, \cdots, N-1$) and Δt is the sampling interval. Eq. (9) shows that the power spectrum $S(f)$ carries all the information relevant to the time correlation function $C(t)$ and elucidates its behavior in the frequency domain. Therefore $S(f)$ can reveal insight into dynamic character and time scales of the system. For example, in the case of Debye relaxation given by single-exponential decay, $S(f)$ is a Lorentzian that decreases as $1/f^2$ at high frequencies. If the system is characterized by multiple relaxation times, say, f_1^{-1} and f_2^{-1} (with $f_1 \ll f_2$), its power spectrum displays a plateau in the low frequency region ($f \ll f_1$) and $1/f^2$ decay in the high frequency limit $f \gg f_2$. In the intermediate region $f_1 \ll f \ll f_2$, $S(f)$ varies approximately as $1/f$.[32]

III. SIMULATION METHODS

The simulation cell is comprised of a rigid diatomic solute immersed in $\text{EMI}^+\text{PF}_6^-$, consisting of 112 pairs of rigid cations and anions. We consider two different solute charge distributions: a neutral pair (NP) without charges and an ion pair (IP) with unit charge separation. When solvent dynamics occurs in the presence of NP, i.e. NP is the active electronic state, IP is regarded as the reference electronic state, and vice versa. The Lennard-Jones (LJ) parameters employed for each constituent atom of the solute are $\sigma = 4\,\text{Å}$ and $\epsilon/k_B = 100\,\text{K}$ (with the Boltzmann constant k_B). Its bond length remains fixed at

3.5 Å for all cases considered here. As for the solvent interaction potential, we employ the same parametrization as in Ref. 33.

MD simulations were conducted in the canonical ensemble at temperature $T = 400\,\text{K}$ through the use of the DL_POLY program.[34] For each solute charge distribution, we simulated the combined solute-solvent system for $70\,\text{ns}$ after $6\,\text{ns}$ equilibration. To compute the power spectrum of the energy gap with reduced noise, we divided the trajectory into seven $10\,\text{ns}$ segments and calculated $S(f)$ in Eq. (10) by averaging over the seven segments. The sampling time interval Δt in our simulations was $10\,\text{fs}$, which sets the maximum frequency of our power spectrum analysis at $50\,\text{ps}^{-1}$, while the minimum is $10^{-4}\,\text{ps}^{-1}$.

For comparison, we also performed simulations in aprotic acetonitrile at $T = 300\,\text{K}$. In the simulation cell, a single NP (or IP) solute is immersed in 512 rigid molecules of acetonitrile. The LJ parameters and partial charges for acetonitrile were taken from Ref. 35. The trajectory was $20\,\text{ns}$ long and the FC energy gap was saved at every $2\,\text{fs}$.

IV. TIME CORRELATION FUNCTION AND POWER SPECTRUM

In this section, we present MD results for equilibrium solvation dynamics in $\text{EMI}^+\text{PF}_6^-$ and acetonitrile. We begin with the time correlation functions of the FC energy gap fluctuations in the presence of the NP and IP solutes in Fig. 1.

The MD results for $C_{a/r}(t)$ in $\text{EMI}^+\text{PF}_6^-$ exhibit biphasic relaxation, i.e., ultrafast inertial relaxation followed by an extremely slow decay [Fig. 1(a) and (b)], consonant with prior simulation studies.[1,2,3,4,6,7,8] Long-time behaviors of $C_{a/r}(t)$ are well described by the stretched exponential function $\exp[-(t/\tau_0)^\beta]$:[1,4,7] A good agreement with the MD results was obtained with fitting parameters $\beta = 0.30$ and $\tau_0 = 1.75\,\text{ps}$ for $1\,\text{ps} \lesssim t \lesssim 50\,\text{ps}$ in the case of NP. For IP, the stretched exponential fit with $\beta = 0.18$ and $\tau_0 = 16.84\,\text{ps}$ applies to a time range, $1\,\text{ps} \lesssim t \lesssim 1000\,\text{ps}$, which is about 20 times wider than the NP case. The result that the τ_0 value with IP is larger than that with NP by one order of magnitude is a direct consequence of slow solvent relaxation dynamics in the presence of the former solute, compared with the latter. For instance, the $C_{a/r}(t)$ value reduces to below 0.1 after $t \gtrsim 1\,\text{ns}$ in the presence of IP, whereas it takes much shorter $\sim 34\,\text{ps}$ with NP. The corresponding solvation times are $\tau_{\text{solv}} = 450$ and $11\,\text{ps}$ for the IP and NP solutes, respectively.

For comparison, we consider $C_{a/r}(t)$ in acetonitrile in Fig. 1(c) and (d). We notice that solvation dynamics in acetonitrile are much faster than those in $\text{EMI}^+\text{PF}_6^-$, congruent with previous studies. The MD results for τ_{solv} for NP and IP are 0.17 and $0.29\,\text{ps}$, which are smaller than the $\text{EMI}^+\text{PF}_6^-$ values by 2–3 orders of magnitude. The biexponential functions $c\exp(-t/t_1) + (1 - c)\exp(-t/t_2)$ with $c = 0.97$, $t_1 = 0.14\,\text{ps}$, $t_2 = 1.086\,\text{ps}$ for NP and $c = 0.85$, $t_1 = 0.09\,\text{ps}$, $t_2 = 1.31\,\text{ps}$ for IP provide excellent fits for $C_{a/r}(t)$ in acetonitrile for $t \gtrsim 1\,\text{ps}$. As analyzed below, $S_{a/r}(f)$ associated with $C_{a/r}(t)$ in acetonitrile does not show pronounced $1/f$ behavior. Thus while a stretched exponential function also appears to yield a reasonable fit (result not shown here), we will take the view that $C_{a/r}(t)$ in acetonitrile is biexponential with two relaxation times. In the long-time limit of this description, $C_{a/r}(t)$ becomes a single exponential decay characterized by the longer of the two relaxation times.

To gain additional insight into characteristics of equilibrium solvation dynamics, we consider the power spectrum $S_{a/r}(f)$ of the fluctuating FC energy gap $\Delta E_{a \to r}(t)$. Figure 2 presents $S_{a/r}(f)$ in $\text{EMI}^+\text{PF}_6^-$ and in acetonitrile, obtained from MD simulations with the aid of Eq. (10). We observe in Fig. 2(a) that $S_{a/r}(f)$ of NP in $\text{EMI}^+\text{PF}_6^-$ is characterized by at least four different regimes:[18,19,32] In the low frequency region below $0.001\,\text{ps}^{-1}$, the spectrum is of a white-noise type, which reveals the absence of correlation between two events separated by longer than $\sim 1\,\text{ns}$. For later use, we denote as f_c ("crossover frequency") the frequency below which $S_{a/r}(f)$ flattens out. For the NP solute under consideration here, $f_c \approx 10^{-3}\,\text{ps}^{-1}$. As f increases above f_c, the power spectrum exhibits the $1/f$ behavior, which is often interpreted as the presence of many different relaxation time scales.[32] If the frequency further increases beyond $\sim 1\,\text{ps}^{-1}$, $S_{a/r}(f)$ begins to drop sharply. This is attributed to the rapid initial decay of $C_{a/r}(t)$ at short times [cf. Fig. 1(a)]. Finally, in the high frequency region $f \gtrsim 10\,\text{ps}^{-1}$, the power spectrum decreases as $\sim 1/f^2$. For perspective, the reader is reminded that $f = 10^{-4}\,\text{ps}^{-1}$ and $50\,\text{ps}^{-1}$ are the lower and upper limits of our analysis of the MD results in the frequency domain.

The power spectrum for IP in $\text{EMI}^+\text{PF}_6^-$ in Fig. 2(b), though similar to that for NP, shows a couple of interesting differences. First, we were not able to observe a white-noise spectrum in the low frequency region of $S_{a/r}(f)$ in the presence of IP. The most likely reason is that the MD trajectory is not long enough to probe the onset of the complete loss of correlations because $C_{a/r}(t)$ in the IP case decays much more slowly than that in the NP case. We ascribe this difference in $C_{a/r}(t)$ to electrostriction. To be specific, it tends to enhance the solvation structure around IP compared to NP and in turn makes rugged the landscape of the potential energy surface, upon which solvent ions diffuse.[1] This leads to slower diffusion of solvent ions and therefore slower relaxation of ΔE fluctuations in the presence of IP than NP. We thus expect that the white-noise plateau for the former solute will appear at frequencies lower than $10^{-4}\,\text{ps}^{-1}$. This means that f_c for IP would be lower than f_c for NP, $10^{-3}\,\text{ps}^{-1}$, by more than one decade. Second, $S_{a/r}(f)$ with IP shows a flat region for

$0.1\,\mathrm{ps}^{-1} \lesssim f \lesssim 1\,\mathrm{ps}^{-1}$. While $S_{a/r}(f)$ with NP also has a hint of a plateau around $f = 1\,\mathrm{ps}^{-1}$, it is much more prominent in the case of IP. The plateau is a part of the Gaussian power spectrum associated with the ultrafast initial relaxation of $C_{a/r}(t)$. One quick and easy way to see this is that infinitely fast delta function relaxation yields a plateau in the frequency domain. This plateau is more noticeable in IP because the difference in time scales between its inertial and diffusive dynamics is larger than that of NP.

The power spectra of the stretched exponential fits in $\mathrm{EMI}^+\mathrm{PF}_6^-$ are compared with the MD results in Fig. 2(a) and (b). For both IP and NP, the stretched exponential functions well describe the $1/f$ characteristics—both the range and exponent of the power law behavior—of the simulation results. One prevalent notion is that stretched exponential behavior arises from the superposition of different single exponential decays, weighted by a broad distribution of relaxation times.[36] While the assumption of single exponentials per se may be too restrictive, there is considerable evidence that RTIL dynamics are characterized by a distribution of different time scales.[37,38,39,40,41] As pointed out in Sec. II, the power spectrum of the system, involving a number of relaxation processes of different time scales, in general exhibits $1/f$ dependence.[32] Thus the presence of the $1/f$-type domain in the power spectrum of ΔE is another manifestation of non-exponential RTIL relaxation. This also suggests the similarity between solvation dynamics in the RTILs and the dynamic heterogeneity observed in glassy liquids.[42,43,44]

Before we turn to memory functions, we briefly consider $S_{a/r}(f)$ for acetonitrile in Figure 2(c) and (d). In the case of NP, $S_{a/r}(f)$ displays a white-noise plateau for $f \lesssim 2\,\mathrm{ps}^{-1}$ but it does not show a $1/f$ power-law behavior. For IP, the white-noise spectrum obtains for $f \lesssim 0.08\,\mathrm{ps}^{-1}$. As f increases beyond the white-noise region, $S_{a/r}(f)$ briefly shows $1/f^\alpha$ behavior with $\alpha \simeq 0.53$ before it begins a rapid decrease. As in $\mathrm{EMI}^+\mathrm{PF}_6^-$, the crossover frequency f_c for IP is smaller than that for NP, again due to electrostriction. Regardless of the solute charge distributions, the onset of the white-noise region is at much higher frequencies in acetonitrile than in $\mathrm{EMI}^+\mathrm{PF}_6^-$ because the long-time solvent relaxation in the former is much faster than that in the latter. Furthermore, the $1/f$ spectrum is nearly absent in $S_{a/r}(f)$ of acetonitrile in contrast to the $\mathrm{EMI}^+\mathrm{PF}_6^-$ case. As mentioned above, this is why we favor a biexponential description for $C_{a/r}(t)$ in acetonitrile over a stretched exponential description. We notice that except for the rapid decrease in the neighborhood of $f = 10\,\mathrm{ps}^{-1}$ arising from ultrafast inertial relaxation of $C_{a/r}(t)$, the biexponential functions indeed provide an excellent framework to describe $S_{a/r}(f)$ in acetonitrile.

V. MEMORY FUNCTION ANALYSIS

Here we consider a simple model description for $S(f)$ and analyze its memory function $\zeta(t)$ to gain insight into long-time solvation dynamics. As observed above, power spectra in $\mathrm{EMI}^+\mathrm{PF}_6^-$ are characterized by at least four different regimes; viz., $S(f)$ generally show white-noise, $1/f$, sharp fall-off and $1/f^2$ behaviors in turn as the frequency increases. Since we are mainly interested in long-time dynamics, we ignore the frequency region (i.e., $1\,\mathrm{ps}^{-1} \lesssim f \lesssim 10\,\mathrm{ps}^{-1}$) of rapid $S(f)$ decay, which arises mainly from ultrafast inertial relaxation of $C(t)$. We thus consider the power spectrum of the following form:

$$
S(\omega) = \begin{cases}
A\omega_c^{-1} & \text{for } 0 < \omega < \omega_c \ , \\
A\omega^{-1} & \text{for } \omega_c < \omega < \omega_0 \ , \\
A\omega_0\omega^{-2} & \text{for } \omega_0 < \omega < \omega_m \ , \\
0 & \text{for } \omega > \omega_m \ ,
\end{cases} \tag{11}
$$

where $S(-\omega) = S(\omega)$, $\omega \equiv 2\pi f$ and A is the normalization constant given by $2A \equiv [2 - \omega_0/\omega_m + \ln(\omega_0/\omega_c)]^{-1}$. By differentiating Eq. (9) twice with respect to t and setting $t = 0$, we derive a sum rule[29]

$$
\omega_s^2 = \int_{-\infty}^{\infty} d\omega\, \omega^2 S(\omega) = \frac{\omega_0\omega_m - \omega_0^2/2 - \omega_c^2/6}{2 - \omega_0/\omega_m + \ln(\omega_0/\omega_c)}, \tag{12}
$$

which clearly shows the necessity of a high frequency cutoff at ω_m in Eq. (11).

The parameters employed to model $S(f)$ are compiled in Table I. S1 and S2 there are the model descriptions for solvation of NP and IP in $\mathrm{EMI}^+\mathrm{PF}_6^-$, respectively, while the corresponding cases in acetonitrile are modeled by S3 and S4. Thus S1 to S4 correspond to the cases in Fig. 2(a) to (d), respectively. The solvent frequency ω_s was obtained from the simulations via Eq. (3) and the cutoff frequency ω_m was estimated from Eq. (12). The values of ω_c and ω_0 were determined with the aid of the MD results in Fig. 2. In the presence of IP in $\mathrm{EMI}^+\mathrm{PF}_6^-$, we were not able to obtain ω_c from the simulation because the plateau behavior in the low frequency region of $S(f)$ was not accessible as mentioned above [Fig. 2(b)]. In the absence of any additional information on the crossover frequency, we assumed $\omega_c = 2\pi \times 10^{-4}\,\mathrm{ps}^{-1}$, the lowest frequency that is allowed in our analysis of MD results, for S2. The corresponding crossover frequency for S1, viz., NP in $\mathrm{EMI}^+\mathrm{PF}_6^-$, is $\omega_c \approx 2\pi \times 10^{-3}\,\mathrm{ps}^{-1}$. For S3, we employed $\omega_c = \omega_0$ because acetonitrile does not exhibit a $1/f$ spectrum in the presence of NP. The narrow $1/f$ region present in S4 was incorporated into the model calculations by choosing $\omega_c = 0.16\pi\,\mathrm{ps}^{-1}$ and $\omega_0 = 4\pi\,\mathrm{ps}^{-1}$.

Within the model description of Eq. (11), we can determine $\zeta(t)$ exactly. Specifically, we make Laplace trans-

form of Eq. (9) with Eq. (11) to find

$$
\begin{aligned}
\tilde{C}(z) &= \int_{-\infty}^{\infty} d\omega\, S(\omega)\frac{z}{\omega^2 + z^2} \\
&= 2A\left[\int_0^{\omega_c} d\omega\frac{z}{\omega_c(\omega^2+z^2)} + \int_{\omega_c}^{\omega_0} d\omega\frac{z}{\omega(\omega^2+z^2)} \right. \\
&\qquad \left. + \int_{\omega_0}^{\omega_m} d\omega\frac{\omega_0 z}{\omega^2(\omega^2+z^2)}\right] \\
&= 2A\left[\frac{1}{\omega_c}\tan^{-1}\frac{\omega_c}{z} + \frac{1}{2z}\left(\ln\frac{\omega_0^2}{\omega_0^2+z^2}\right.\right. \\
&\qquad \left. -\ln\frac{\omega_c^2}{\omega_c^2+z^2}\right) + \frac{\omega_0}{z}\left(\frac{1}{\omega_0}-\frac{1}{\omega_m}\right) \\
&\qquad \left. + \frac{\omega_0}{z^2}\left(\tan^{-1}\frac{\omega_0}{z}-\tan^{-1}\frac{\omega_m}{z}\right)\right] .
\end{aligned}
\tag{13}
$$

We rewrite Eq. (7) as

$$
\tilde{\zeta}(z) = \omega_s^2\frac{\tilde{C}(z)}{1 - z\tilde{C}(z)} - z ,
\tag{14}
$$

substitute Eq. (13) into Eq. (14) and make inverse Laplace transform[45] numerically to obtain $\zeta(t)$.

Figure 3(a) displays the results for the memory function $\zeta(t)$ thus obtained. For comparison, we employ the method used in Ref. 4 to determine $\zeta(t)$ directly from $C(t)$ and associated time correlation functions of a nonconservative force[46] and present the results in Figure 3(b). We notice in Figure 3(a) that $\zeta(t)$ falls off very quickly at the very early stage of relaxation, regardless of the crossover frequency ω_c. Subsequent decay of the residual memory varies strongly with ω_c. Generally, the long-time relaxation of $\zeta(t)$ becomes slower with decreasing ω_c.[47] Comparison of the results in Figure 3(a) and (b) shows that while there are differences, $\zeta(t)$ obtained from model $S(\omega)$ in Eq. (11) correctly captures important features of memory both at the qualitative and semi-quantitative level. These include rapid initial decay of a large amplitude and the existence of a long-time tail. Nonetheless, the model calculations yield spurious oscillations at short times (see below) and overestimation of the long-time memory effect. For example, the model predictions for the magnitude of the residual memory, say at $t \approx 1$ ps, are considerably larger than the MD results. This overestimation is attributed mainly to the neglect of the rapid decay of $S(f)$ in our model description at high frequencies.

Here we briefly examine the oscillatory behavior of $\zeta(t)$ observed in the first few hundred femtoseconds in Fig. 3(a). It is of interest to note that the period of these oscillations is close to $2\pi/\omega_m$. This suggests that oscillations are closely linked to the presence of a cutoff at frequency ω_m in the model power spectrum employed in this study. To check this, we considered a Gaussian power spectrum $S(f) = (A/\omega_0)\exp[-(\omega-\omega_0)^2/2\omega_g^2]$ for $\omega > \omega_0$ that does not require a high-frequency cutoff. The resulting friction is exhibited in Fig. 4. The disappearance of the rapid initial oscillations confirms that

indeed the cutoff is mainly responsible for rapid oscillations in $\zeta(t)$ in Fig. 3(a). We note that slow oscillations in Fig. 4 arise from the discontinuity in the derivative of the model Gaussian spectrum at $\omega = \omega_0$.

Finally, we consider solvation time $\tau_{\text{solv}}(= \tilde{C}(0))$. It is related to the total memory $\tilde{\zeta}(0)$ via Eq. (7), so that

$$
\frac{\tilde{\zeta}(0)}{\omega_s^2} = \tau_{\text{solv}} = \frac{\pi}{2\omega_c}\left(2 - \frac{\omega_0}{\omega_m} + \ln\frac{\omega_0}{\omega_c}\right)^{-1} ,
\tag{15}
$$

where we have used Eq. (13) in passage to the final expression. The results for τ_{solv} obtained from Eq. (15) are presented in Table I. We notice that τ_{solv} is inversely proportional to the crossover frequency ω_c. Thus, all other things being equal, τ_{solv} increases as ω_c decreases. This is directly related to the observation made above that long-time relaxation of $\zeta(t)$ becomes slower with decreasing ω_c. Also interesting is that τ_{solv} varies with the frequency range ω_0/ω_c associated with the $1/f$ behavior in $S(f)$. For instance, for given ω_c, the growing range of the $1/f$ region, i.e., increasing ω_0, tends to reduce the solvation time. Since the lower limit of distributed time scales for $1/f$ is $\sim \omega_0^{-1}$ [cf. Eq. (11)], the shortest time scale for $1/f$ becomes faster as ω_0 increases. In other words, faster processes become available increasingly more to the system, while the availability of slower processes remains unchanged. This yields the reduction in the solvation time because contributions to solvent relaxation from faster processes become progressively more important than slower processes.

VI. CONCLUSIONS

We have studied the time correlation functions and power spectra of the FC energy gap and related memory functions associated with solvation dynamics of model diatomic solutes in $\text{EMI}^+\text{PF}_6^-$ and CH_3CN. It was found that the power spectra of both the NP and IP solutes in $\text{EMI}^+\text{PF}_6^-$ display $1/f$ dependence over a range of intermediate frequencies, which indicates nonexponential relaxation dynamics in RTILs. In the case of NP, we observed white-noise behavior at low frequencies. The power spectrum of NP in acetonitrile does not yield the $1/f$ dependence and its crossover frequency is much higher than the corresponding value in $\text{EMI}^+\text{PF}_6^-$. Though not pronounced, the IP solute in acetonitrile shows $1/f$ dependence but in a frequency range much narrower than that in $\text{EMI}^+\text{PF}_6^-$.

Using a simple but analytic model for power spectra, we have determined the memory function in the GLE description of solvation dynamics and compared with the MD results. With proper account of white-noise, $1/f$ and $1/f^2$ behaviors of power spectra, we have found that the model description reproduces the MD results of friction reasonably well. We have also found that the time scale of memory effects and the $1/f$ regime are closely related. We have obtained the solvation time in terms of

the frequency parameters of the model power spectrum description. Among others, the solvation time was found to be inversely proportional to the crossover frequency. Together with our MD results of $S_{a/r}(f)$, this indicates that the solvation time for the IP solute in $EMI^+PF_6^-$ is far longer than that for NP, at least by one order of magnitude. Electrostriction which exerts a strong influence on the landscape of the potential energy surface relevant to solvent ion diffusion is mainly responsible for the variation of solvation time with the solute charge distribution.

* Author to whom correspondence should be addressed. E-mail: yjjung@snu.ac.kr

[1] Y. Shim, J. Duan, M. Y. Choi, and H. J. Kim, J. Chem. Phys. **119**, 6411 (2003).

[2] C. J. Margulis, Mol. Phys. **102**, 829 (2004).

[3] M. N. Kobrak and Z. Znamenskiy, Chem. Phys. Lett. **395**, 127 (2004).

[4] Y. Shim, M. Y. Choi, and H. J. Kim, J. Chem. Phys. **122**, 044511 (2005).

[5] B. L. Bhargava and S. Balasubramanian, J. Chem. Phys. **123**, 144505 (2005).

[6] M. N. Kobrak, J. Chem. Phys. **125**, 064502 (2006).

[7] D. Jeong, Y. Shim, M. Y. Choi, and H. J. Kim, J. Phys. Chem. B **111**, 4920 (2007).

[8] Y. Shim, D. Jeong, S. Manjari, M. Y. Choi, and H. J. Kim, Acc. Chem. Res. **40**, 1130 (2007).

[9] M. N. Kobrak, J. Chem. Phys. **127**, 184507 (2007).

[10] R. Karmakar and A. Samanta, J. Phys. Chem. A **106**, 4447 (2002); **106**, 6670 (2002); **107**, 7340 (2003); A. Samanta, J. Phys. Chem. B **110**, 13704 (2006).

[11] J. A. Ingram, R. S. Moog, N. Ito, R. Biswas and M. Maroncelli, J. Phys. Chem. B **107**, 5926 (2003); N. Ito, S. Arzhantsev, and M. Maroncelli, Chem. Phys. Lett. **396**, 83 (2004); S. Arzhantsev, H. Jin, N. Ito, and M. Maroncelli, Chem. Phys. Lett. **417**, 524 (2006); S. Arzhantsev, H. Jin, G. A. Baker, and M. Maroncelli, J. Phys. Chem. B **111**, 4978 (2007); H. Jin, G. A. Baker, S. Arzhantsev, J. Dong, and M. Maroncelli, J. Phys. Chem. B **111**, 7291 (2007).

[12] D. Chakrabarty, P. Hazra, A. Chakarborty, D. Seth, and N. Sarkar, Chem. Phys. Lett. **381**, 697 (2003).

[13] P. K. Chowdhury, M. Halder, L. Sanders, T. Calhoun, J. L. Anderson, D. W. Armstrong, X. Song, and J. W. Petrich, J. Phys. Chem. B **108**, 10245 (2004); L. Sanders Headley, P. Mukherjee, J. L. Anderson, R. Ding, M. Halder, D. W. Armstrong, X. Song and J. W. Petrich, J. Phys. Chem. A **110**, 9549 (2006).

[14] B. Lang, G. Angulo, and E. Vauthey, J. Phys. Chem. A **110**, 7028 (2006).

[15] J. F. Wishart and E. W. Castner, J. Phys. Chem. B **111**, 4639 (2007); A. M. Funston, T. A. Fadeeva, J. F. Wishart, and E. W. Castner, J. Phys. Chem. B **111**, 4963 (2007).

[16] For a very recent exposition of various theoretical and experimental efforts to understand physico-chemical properties of RTILs, see Acc. Chem. Res. **40**, No. 11 (2007); J. Phys. Chem. B **111(18)**, (2007).

[17] Y. Shim and H. J. Kim, J. Phys. Chem. B **111**, 4510 (2007).

[18] M. Sasai, I. Ohmine, and R. Ramaswamy, J. Chem. Phys. **96**, 3045 (1992); A. Mudi, C. Chakravarty, and R. Ramaswamy, J. Chem. Phys. **122**, 104507 (2005).

[19] R. Sharma, A. Mudi, and C. Chakravarty, J. Chem. Phys. **125**, 044705 (2006).

[20] C. Reichhardt and C. J. O. Reichhardt, Phys. Rev. Lett. **90**, 095504 (2003); C. Reichhardt and C. J. O. Reichhardt, Phys. Rev. E **75**, 051407 (2007).

[21] J. T. Hynes, E. A. Carter, G. Ciccotti, H. J. Kim, D. A. Zichi, M. Ferrario and R. Kapral, in *Perspectives in Photosynthesis*, edited by J. Jortner and B. Pullman (Kluwer, Dordrecht, 1990).

[22] E. A. Carter and J. T. Hynes, J. Chem. Phys. **94**, 5961 (1991).

[23] P. A. Egelstaff, Phys. Chem. Liq. **16**, 293 (1987).

[24] G. R. Kneller and K. Hinsen, J. Chem. Phys. **115**, 11097 (2001).

[25] R. K. Sharma, R. K. Moudgil, and K. Tankeshwar, Phys. Rev. E **54**, 3652 (1996).

[26] M. I. Barker and T. Gaskell, J. Phys. C **5**, 353 (1972).

[27] K. Kaneko and T. Konishi, Phys. Rev. A **40**, 6130 (1989).

[28] D. Forster, *Hydrodynamic Fluctuation, Broken Symmetry, and Correlation Functions* (Benjamin, Reading, 1975).

[29] H. L. Friedman, *A Course in Statistical Mechanics* (Prentice-Hall, Englewood Cliffs, 1985).

[30] R. Kubo, M. Toda, and N. Hashitsume, *Nonequilibrium Statistical Mechanics* (Springer-Verlag, Heidelberg, 1991), 2nd ed.

[31] W. H. Press, S. A. Teukolsky, W. T. Vetterling, and B. P. Flannery, *Numeical Recipes in C* (Cambridge University Press, Cambridge, 1992), 2nd ed.

[32] E. Milotti, arxiv.org:physics/0204033.

[33] Y. Shim, M. Y. Choi, and H. J. Kim, J. Chem. Phys. **122**, 044510 (2005).

[34] T. R. Forster and W. Smith, *The DL_POLY_2.13 Reference Manual* (CCLRC, Daresbury Laboratory, Warington, 2001).

[35] D. M. F. Edwards, P. A. Madden, and I. R. McDonald, Mol. Phys. **51**, 1141 (1984).

[36] J. Colmenero, A. Arbe, A. Alegría, M. Monkenbusch and D. Richter, J. Phys.: Condens. Matter **11**, A363 (1999).

[37] M. G. Del Pópolo and G. A. Voth, J. Phys. Chem. B **108**, 1744 (2004).

[38] M. C. C. Ribeiro, Phys. Chem. Chem. Phys. **6**, 771 (2004).

[39] Z. Hu and C. J. Margulis, Proc. Natl. Acad. Sci. U.S.A. **103**, 831 (2006).

[40] Y. Shim, D. Jeong, M. Y. Choi, and H. J. Kim, J. Chem. Phys. **125**, 061102 (2006).

[41] C. Cadena, Q. Zhao, R. Q. Snurr, and E. J. Maginn, J.

Phys. Chem. B **110**, 2821 (2006).

[42] For a recent review, see, e.g., R. Richert, J. Phys.: Condens. Matter **14**, R703 (2002).

[43] For a general review, see, e.g., M. D. Ediger, C. A. Angell and S. R. Nagel, J. Phys. Chem. **100**, 13200 (1996).

[44] F. Alvarez, A. Alegría, and J. Colmenero, Phys. Rev. B **44**, 7306 (1991).

[45] G. Honig and U. Hirdes, J. Comput. Appl. Math. **10**, 113 (1984).

[46] In the numerical inversion of Eq. (14) to the time domain, the linear term in z should be cancelled out by asymptotic behavior of $\omega_s^2 \tilde{C}(z)/[1 - \tilde{C}(z)]$ for large z. Unlike the analytic expression in Eq. (13), however, numerical results of $\tilde{C}(z)$ do not satisfy this condition. We have thus determined $\tilde{\zeta}(z)$ by combining small and large z behaviors obtained from $C(t)$ and from the time correlation function of the nonconservative force, respectively.

[47] We have performed additional calculations by varying ω_c with ω_0 and ω_m fixed and confirmed that $\zeta(t)$ decays more slowly with decreasing ω_c.

	ω_s	$\omega_c/2\pi$	$\omega_0/2\pi$	$\omega_m/2\pi$	τ_{solv}	Solute-solvent
S1	5.82	10^{-3}	1	8.04	28.4	NP-EMI$^+$PF$_6^-$
S2	7.81	10^{-4}	1	17.7	224.1	IP-EMI$^+$PF$_6^-$
S3	10.23	2	2	3.14	0.07	NP-CH$_3$CN
S4	12.99	0.08	2	11.8	0.61	IP-CH$_3$CN

TABLE I: Frequency parameters for the power spectrum in Eq. (11) and the solvation time τ_{solv} given by Eq. (15). The frequency and time are measured in the units of ps^{-1} and ps, respectively. S1 through S4 model the power spectra obtained from MD simulations of solute-solvent systems shown in the last column.
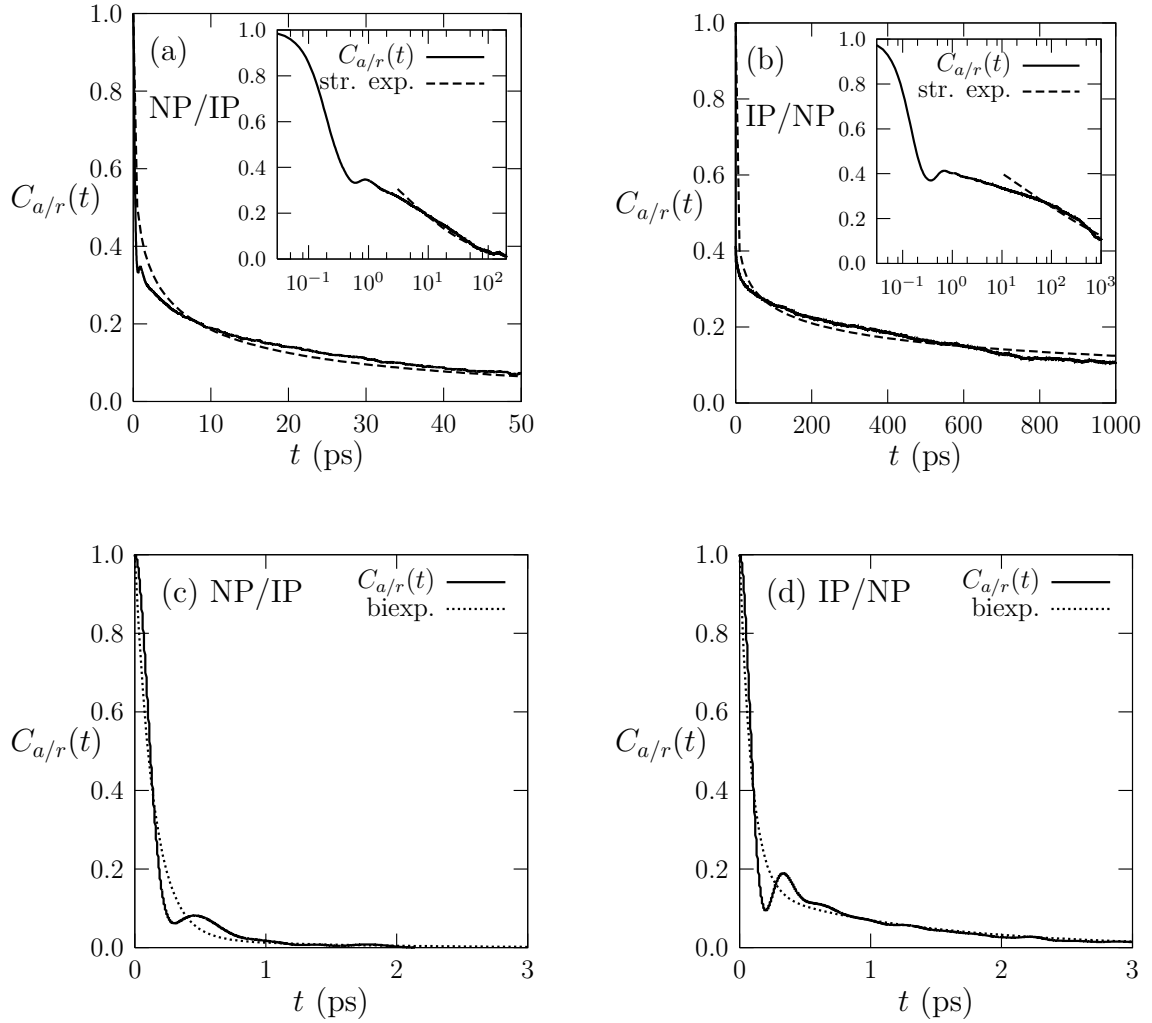

FIG. 1: Time correlation function $C_{a/r}(t)$ of $\delta\Delta E_{a\to r}(t)$ in (a) EMI$^+$PF$_6^-$ for NP/IP, (b) EMI$^+$PF$_6^-$ for IP/NP, (c) CH$_3$CN for NP/IP, and (d) CH$_3$CN for IP/NP active/reference states of the solute. Insets in (a) and (b) display semi-log plots for $C_{a/r}(t)$
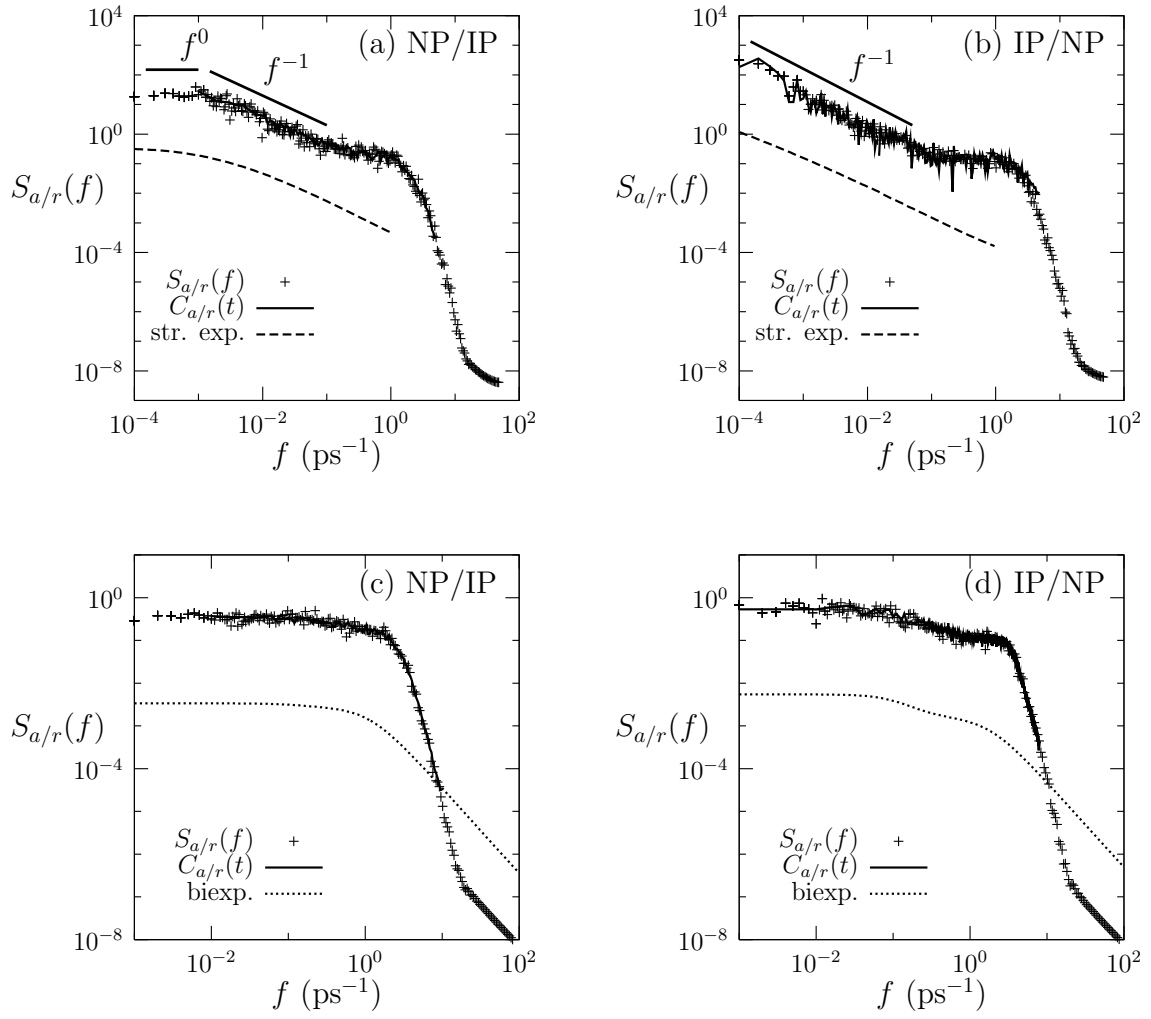
FIG. 2: Power spectrum $S_{a/r}(f)$ of $\delta\Delta E_{a\to r}(t)$. The results obtained via Eq. (10) are plotted in "+" symbols, while the Fourier transforms of $C_{a/r}(t)$ are given in a solid line. They show an excellent agreement as they should. Also displayed are Fourier transforms of the stretched exponential and biexponential fits. (a), (b), (c), and (d) refer to the same cases as in Fig. 1.
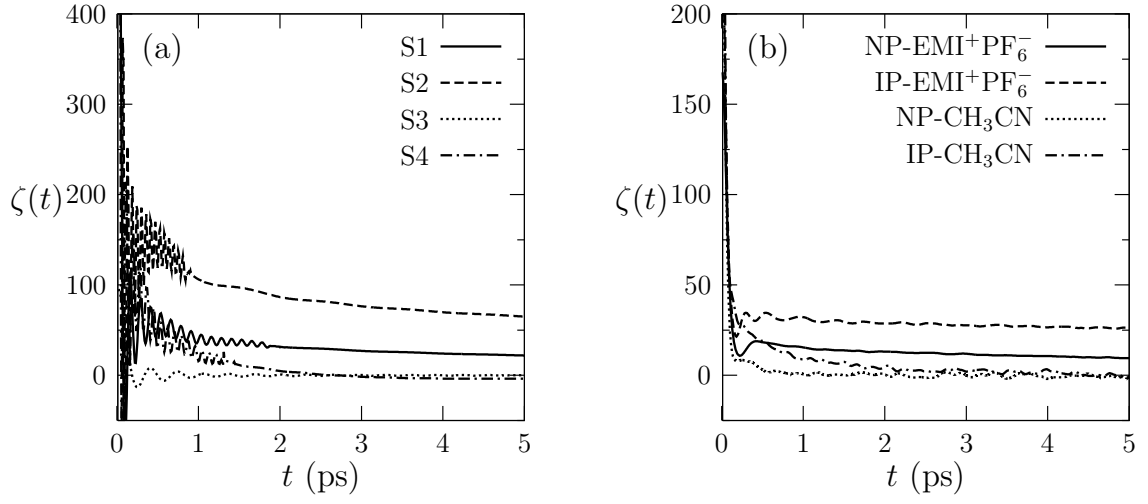
FIG. 3: Memory function $\zeta(t)$, (a) obtained via the inverse transform of Eq. (14), together with Eq. (13) and the parameters for S1 to S4 in Table I; (b) evaluated directly from the correlation function for the NP and IP solutes in $\text{EMI}^+\text{PF}_6^-$ and in acetonitrile.
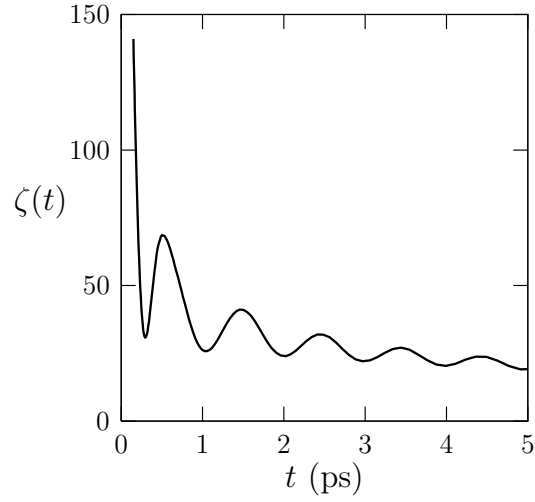

FIG. 4: Memory function $\zeta(t)$ in case that the power spectrum at high frequencies ($\omega > \omega_0$) follows a Gaussian function: $S(\omega) = (A/\omega_0)\exp[-(\omega - \omega_0)^2/2\omega_g^2]$ with $\omega_0 = 2\pi\,\text{ps}^{-1}$ and ω_g set to be $0.8\,\omega_0$. The solvent frequency is given by $\omega_s = 5.7\,\text{ps}^{-1}$ for $\omega_c = 2\pi \times 10^{-3}\,\text{ps}^{-1}$ according to the sum rule.